

Long-wavelength nonpolar phonons in semiconductor heterostructures

F. de León-Pérez^{1,a} and R. Pérez-Alvarez²

¹ Institut für Theoretische Physik III, Universität Stuttgart, Pfaffenwaldring 57, 70550 Stuttgart, Germany

² Physics Faculty, Havana University 10400 Havana, Cuba

Received 21 July 2004

Published online 5 November 2004 – © EDP Sciences, Società Italiana di Fisica, Springer-Verlag 2004

Abstract. Employing a phenomenological long-wavelength approach recently developed, both acoustic and optical phonons in nonpolar heterostructures are studied. Phonon modes in an arbitrary direction can be calculated without additional effort respect to high symmetry directions. A simple analytical expression for the dispersion relation in superlattices guides the physical discussion. We apply this to the calculation of phonon modes in unstrained short period isotopic Ge superlattices, in quantum wells and in strained short period Si/Ge superlattices. We find very good agreement with the results of other, more elaborated and costly calculations.

PACS. 63.20.Dj Phonon states and bands, normal modes, and phonon dispersion – 63.22.+m Phonons or vibrational states in low-dimensional structures and nanoscale materials – 68.65.Cd Superlattices

1 Introduction

The vibrational characteristics of multilayered structures are of both fundamental and practical interest. Optical spectroscopies are suitable for the investigation of semiconductor microstructures, and can also be used to characterize the quality of the heterostructures, in particular the details of the interfaces, for a review see reference [1]. In order to explain the main experimental results, different models have been developed to describe the phonon dispersion curves. These models range from simplified linear chain models [2] to the most elaborate ones based on *ab initio* local-density calculations [3]. Most optical spectroscopies are subject to rather stringent selection rules which arise from wave-vector conservation. In fact, the phonon created or annihilated must have a wave vector of magnitude close to zero, i.e., near the center of the Brillouin zone. For this reason, phenomenological long-wavelength models are successful when compared with experimental results.

Phenomenological long-wavelength models have been widely employed with good results even for relatively short wavelengths. Their mathematical simplicity helps to derive analytical results and visualize the physics of different problems. Acoustic phonons have been widely studied [4–6] with the help of the Christoffel equations [7]. For optical phonons in polar materials a long-wavelength model has been proposed [8] and successfully applied to heterostructures [9]. As a particular case of [8], we can

study phonons in nonpolar semiconductors when the coupling constant between the electric field and the atomic oscillations vanishes [10]. This formulation has allowed the study of high symmetry phonons in quantum wells (QWs) and superlattices (SLs) in strained and unstrained materials, and the interface modes due to the presence of alloys at the interface. Also the influence of the inherent electric field in the vibrational properties of mixed polar-nonpolar heterostructure can be predicted by combining these two approaches [11].

As explained in [8] both models [8,10] contain the Christoffel equations for acoustic phonons as a particular case with the right selection of the input parameters. We showed in [12] that the model for optical phonons is a counterpart of that corresponding to acoustic phonons; and considering both together the best results comparing with other methods and experimental data are obtained. In the present paper both acoustic and optical phonons in nonpolar heterostructures are studied employing the same long-wavelength approach of reference [10]. We analyze here the coupled longitudinal and transverse atomic oscillations.

Note that in previous works only analytical expressions for uncoupled modes could be reported [10]. The coupled modes have been studied only indirectly through phonon tunneling [12], exploiting the relation between transmission and reflection characteristics and phonon properties. Starting from this model to study phonons in heterostructures for arbitrary directions of the reciprocal space two traditional approaches are available: the secular equation and the transfer matrix method. Both have the advantage

^a e-mail: fernando@theo3.physik.uni-stuttgart.de

$$h_j(z) = \begin{pmatrix} i\kappa e^{ik_{Lj}z} & i\kappa e^{-ik_{Lj}z} & -ik_{Tj}e^{ik_{Tj}z} & ik_{Tj}e^{-ik_{Tj}z} \\ ik_{Lj}e^{ik_{Lj}z} & -ik_{Lj}e^{-ik_{Lj}z} & i\kappa e^{ik_{Tj}z} & i\kappa e^{-ik_{Tj}z} \\ 2B_j\kappa k_{Lj}e^{ik_{Lj}z} & -2B_j\kappa k_{Lj}e^{-ik_{Lj}z} & E_j e^{ik_{Tj}z} & E_j e^{-ik_{Tj}z} \\ D_j e^{ik_{Lj}z} & D_j e^{-ik_{Lj}z} & 2B_j\kappa k_{Tj}e^{ik_{Tj}z} & -2B_j\kappa k_{Tj}e^{-ik_{Tj}z} \end{pmatrix}, \quad (3)$$

that the size of the matrix involved does not increase with the size of the system, as is characteristic of the discrete phenomenological models –which are also more complex. Fortunately continuous models also reproduce features for short wavelengths and small systems –i.e. short period superlattices (SL) and short length quantum wells (QWs)– at least in some high symmetry directions. Recently, the eigenmodes in SLs have been studied through linear chains, taking the force constants from ab initio calculations [3], with excellent results. But, to the best of our knowledge this ab initio treatment is developed only for high symmetry directions.

We will show that it is possible to obtain explicit dispersion relations for arbitrary directions of the Brillouin zone in the frame of the continuous model, by employing the transfer matrix formalism. In this way any phonon mode is calculated without additional effort with respect to high symmetry directions. The paper is devoted to study the physics of the less symmetric modes. To the best of our knowledge these results have not been obtained in any previous study [13].

Some nanostructures made up of nonpolar materials with recent scientific interest are studied in this paper, namely isotopic short period Ge SLs and QWs [14], and short period Si/Ge SLs [15]. Isotopic Ge SL means two layers of enriched Ge isotopes repeated periodically. The reason for this selection is the different phonon properties involved. The phonon dispersions of two isotopic enriched Ge bulk materials overlap over a large frequency range (but confined optical modes are still present), and strain effects are not important. On the other hand, in the Si/Ge structures the mechanical vibrations characteristic of each constituent material would not practically penetrate the adjoining slabs. Also homogeneous strain induced by lattice matching to the substrate must be considered.

In the next section the fundamentals of the phenomenological continuum long-wavelength model are briefly described, and the explicit dispersion relations for coupled modes valid for any direction of the wavevector are found. The physical nature of the phonon modes is discussed in Section 3 for the systems of interest and conclusions are presented in Section 4.

2 Phenomenological continuum long-wavelength model

The analytical setup of the phenomenological model can be found in [10,12]. The equations of motion are constituted by three coupled differential equations; which are

obtained from a Lagrangean density that is postulated in the spirit of continuous media. The boundary conditions, continuity of the displacement field \mathbf{u} and the “stress” tensor $\boldsymbol{\sigma}$, are derived straightforwardly from the equations of motion. In a similar way to [8,16] the orthonormality and completeness of the solution space could be proved. An energy balance equation for the energy density flux was found in [12].

A cubic symmetry is sufficient to study the materials here considered [10]. For the solution space of layered structures –where the isotropy in the plane parallel to the growth direction is assumed and the equations of motion are Fourier transformed in that plane– is found [10] that the transverse horizontal (TH) solution is decoupled from the oscillations in the directions y and z – z is the growth direction. Then, transverse (T) and longitudinal (L) independent solutions are coupled. For the transverse wavevector $\kappa = 0$ this subspace is also decoupled into purely longitudinal and transverse vibrations. The decoupled solutions have been intensively studied in [10]. We shall concentrate on finding an analytical expression for the dispersion relation of the coupled modes. The secular equation for layered heterostructures has been discussed in [10] –although it was not reported explicitly. We present it in the Appendix A in order to compare with the simpler expressions developed below. We should emphasize that the order of the secular matrix (4×4 for the QW and 8×8 for the SL) is independent of the linear size of the system. This is advantageous compared with other phonon models for which the order of the secular equation increases with the dimension of the system. Also the long-wavelength model has proved useful not only for long period structures but surprisingly for short period ones [8–10,12].

The relevant information and matrices related to the transfer matrix method –which match \mathbf{u} and $\boldsymbol{\sigma}$ in different layers– are straightforward and presented explicitly in reference [12]. We write below only the transfer matrix for the SL for the sake of completeness in the presentation:

$$T_{SL} = t_b t_w, \quad (1)$$

where

$$t_j(d_j) = h_j(d_j) h_j^{-1}(0), \quad (2)$$

$j = w, b$ label the well and barrier material of width d_j respectively, and

see equation (3) above,

$$B_j = \rho_j \beta_{Tj}^2, \quad (4)$$

$$D_j = \rho_j (\kappa^2 (\beta_{Lj}^2 - 2\beta_{Tj}^2) + \beta_{Lj}^2 k_{Lj}^2), \quad (5)$$

$$E_j = \rho_j \beta_{Tj}^2 (\kappa^2 - k_{Tj}^2), \quad (6)$$

$$k_{L_j(T_j)} = \sqrt{\frac{\omega_{L_j(T_j)}^2(\Gamma) - \omega^2}{\beta_{L_j(T_j)}^2} - \kappa^2}. \quad (7)$$

The elements of the matrix T_{SL} , named T_{ij} in the following, are easily obtained and handled, but given their extension they are not reported here.

With the help of the Bloch theorem we can calculate the dispersion relation and eigenvectors of the infinite SL writing the secular equation in the form

$$(I_4 e^{iqd} - T_{SL}) W = 0, \quad (8)$$

where W represents the fields \mathbf{u} and $\sigma_z = \boldsymbol{\sigma} \cdot \hat{e}_z$, written in the form of column matrix, is

$$W(z) = \begin{bmatrix} \mathbf{u}^t \\ \sigma_z \end{bmatrix}, \quad (9)$$

where q is the SL wavevector, $d = d_w + d_b$ is the SL period and I_4 is the four order identity matrix.

We shall write the SL dispersion relation in a more compact form. For this it is convenient to rewrite the matrices of (8) in the form of 2×2 block matrices, i.e.

$$T_{SL} = \begin{pmatrix} T_1 & T_2 \\ T_3 & T_4 \end{pmatrix}, \quad W = \begin{pmatrix} W_1 \\ W_2 \end{pmatrix}. \quad (10)$$

Replacing these relations in (8) we find two matricial equations for W_1 and W_2 . We combine both equations and obtain after some transformations

$$[I_2 e^{iqd} + Q e^{-iqd} - P] W_1 = 0, \quad (11)$$

where

$$P = T_1 + T_2 T_4 T_2^{-1}, \quad (12)$$

$$Q = T_2 T_4 T_2^{-1} T_1 - T_2 T_3. \quad (13)$$

The determinant of (11) is set equal to zero in order to obtain a non trivial solution. In the calculations we should note that the diagonal (non-diagonal) elements in the submatrices T_i are pure real (imaginary). This property guarantees that the expression to be presently obtained is real. The property $\det(Q) = \det(T_{SL}) = 1$ is also employed –The identity $\det(T_{SL}) = \det(h_b) \det(h_b^{-1}) \det(h_w) \det(h_w^{-1})$ and the fact that $\det(h_i(z))$ is independent of z , as could be seen from (3), lead to $\det(T_{SL}) = 1$. After a straightforward algebra the following dispersion relation is found from the real part of (11)

$$\cos(qd) = \left(B \pm \sqrt{B^2 - 16C + 32} \right) / 8, \quad (14)$$

where

$$B = \text{tr}(P) + \text{tr}(PQ^{-1}), \quad (15)$$

$$C = \text{tr}(Q) + \det(P). \quad (16)$$

The imaginary part of (11) leads to the additional condition $\text{tr}(P) = \text{tr}(PQ^{-1})$, which simplifies the mathematical expression of B . The study shows that this equality does not imply new physical conditions for the vibrational modes neither the appearance of additional modes with particular characteristics. It is also possible to simplify the analytical expression of C after an straightforward algebra. We obtain finally for B and C

$$B = 2 \text{tr}(P), \quad (17)$$

$$C = \Delta = \Delta_{12} + \Delta_{13} + \Delta_{14} + \Delta_{23} + \Delta_{24} + \Delta_{34}, \quad (18)$$

where

$$\Delta_{ij} = \det \begin{pmatrix} T_{ii} & T_{ij} \\ T_{ji} & T_{jj} \end{pmatrix}, \quad (19)$$

and T_{ik} are the elements of the matrix T_{SL} (1).

The expression (14) is much simpler than the traditional 8×8 secular, given in the appendix matrix (25), due to the fact that at the end of the calculations B and C are reduced to elementary expressions of some elements of matrix T_{SL} . All the terms are real, avoiding the tedious diagonalization of the real and imaginary parts of the secular matrix. This simplifies considerably the numerical work. Equation (14) is similar to the dispersion relation of the decoupled modes and the results of [10] for uncoupled modes are recovered for $\kappa = 0$. The coupled modes are now characterized according to the $+/-$ sign in front of the radical. We shall label these in the following as $+$ and $-$ modes respectively. This equation is numerically discussed below. In a similar way it is possible to write a more compact dispersion relation for the QW case.

3 Numerical results and discussion

3.1 Isotopic germanium superlattices

We carefully compared the numerical results using the secular equation (25) and the explicit dispersion relation (14) and did not find differences for the whole range of wave vectors studied. The speed of the computation experiences a significant increment for the later treatment. It is also easier to detect the zeros of the dispersion relation given the considerable simplification of the analytical expressions.

For the ^{70}Ge (^{74}Ge) atom we have used the same parameters as in [10,12,17]. For acoustic phonons we rescale by the isotope mass the sound velocities for natural Ge given in the next subsection. We shall study here the symmetric (^{70}Ge) $_4$ - (^{74}Ge) $_4$ SL reported by other authors [14].

The dispersion relations in some interesting regions are presented in Figure 1. For the [001] direction in Figure 1c –where pure longitudinal (transverse) modes are represented with solid (dashed) lines– we showed in [12] that studying at the same time the optical and acoustic phonons the results of the calculations are improved. A good coincidence with other theoretical and experimental

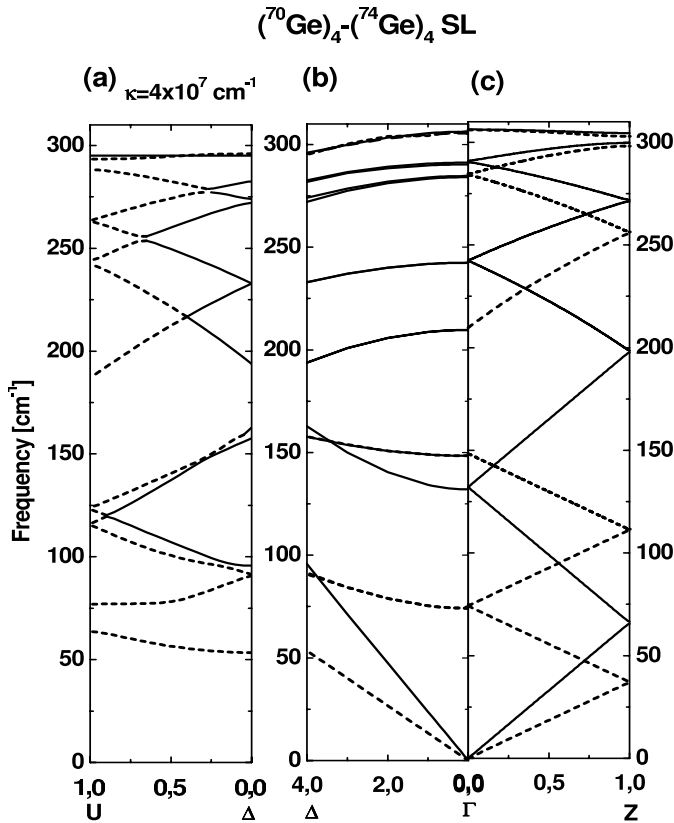


Fig. 1. Phonon dispersion relation for the $(^{70}\text{Ge})_4-(^{74}\text{Ge})_4$ SL. Frequency and wavevectors in cm^{-1} . With solid (dashed) lines we represent in (a) and (b) the + (–) modes, and in (c) the pure L (T) modes. The TH branches are represented with dashed lines. The SL wavevector q in (a) and (c) is normalized to unity (π/d , d is the SL period). (a) Direction ΔU . For the fixed value $\kappa = 4 \times 10^7 \text{ cm}^{-1}$ the phonon branches are plotted as functions of q . The TH modes are not shown. (b) Uncoupled and TH modes as functions of the transverse wavevector κ [$\times 10^7 \text{ cm}^{-1}$] for $q = 0$, direction $[010]$. The modes for a $(^{70}\text{Ge})_4$ QW, represented with dotted lines, are indistinguishable from the topmost superlattices modes, as expected. (c) Dispersion relation in the direction $[001]$ for L and double degenerate T modes. See text for details.

results [14,17] is found for the whole Brillouin zone in this direction (i.e. independently of the wavelength).

The phonon dispersion in the direction $\Gamma\Delta$ of the Brillouin zone ($q = 0$) is presented in Figure 1b. To the best of our knowledge there is no calculations of phonon modes in isotopic SL available for $\kappa \neq 0$, but the following expected qualitative facts help to validate our results. The branches are plotted as function of κ from $\kappa = 0$ to $\kappa = 4 \times 10^7 \text{ cm}^{-1}$, i.e. about 1/3 of the Brillouin zone ($1.11 \times 10^8 \text{ cm}^{-1}$). The selected region is about the same order of magnitude as in Figure 1c, where excellent results were obtained. The acoustic and optical curves do not overlap. In the next subsection the atomic oscillations for a Si/Ge SL in the same direction $[010]$ are satisfacto-

rily compared with other theoretical results. Both systems show the same general trends.

Figure 1b shows both TH and coupled vibrations. The longitudinal modes and the degenerate T modes in $q, \kappa = 0$ retain almost the same character for $\kappa \neq 0$. In particular the TH (represented with dashed lines) and coupled quasi transverse modes are practically undistinguished. We also note a strong influence in the behavior of all these modes of the bulk dispersion relation, given for the parabolic (linear) behavior of the optical (acoustic) branches. The reason for these trends is that the oscillations with longest wavelength do not “detect” the change in symmetry in the grown direction –the cubic symmetry of the host material is replaced for the orthorhombic symmetry of the SL. The branches are less dispersive than in the direction ΓZ .

We also studied a ^{70}Ge QW with ^{74}Ge barriers. The frequency values for the modes confined in the ^{70}Ge QW are plotted in Figure 1b with dotted lines. These curves practically overlap with the topmost optical modes in the SL as for $\kappa = 0$ (see the discussion about in [10,14,17]), and are not further discussed here.

The branches of coupled oscillations are represented in Figure 1b according to the modes of equation (14). The dashed (solid) lines characterize the + (–) modes. The same criterion is used in Figure 1a, where the dispersion relation is plotted in the lower symmetry direction ΔU . For Figure 1a we started from the Δ point in Figure 1b ($\kappa = 4 \times 10^7 \text{ cm}^{-1}$) and calculated the phonon modes as a function of the SL wavevector q . It is interesting to note that the + (–) modes retain the same character in the direction $\Gamma\Delta$ and change in the direction ΔU –where some anticrossings as a function of the SL wavevector q appear. This reflects the fact that the + (–) modes are related to the SL symmetry. The + (–) modes are a proper linear transformation of the longitudinal and transverse independent solutions that diagonalize in blocks the SL matrix. For the uncoupled modes of Figure 1c it is possible to choose between the L and T modes (more illustrative in this situation) and the + (–) modes. In the last case the + (–) modes change continuously from one type to another as a function of q , i.e. similar to Figure 1a but avoiding the anticrossings due to the reduction in the symmetry that for this latter direction is observed.

Figure 1a does not show the TH modes for the sake of clarity. These modes do not present anticrossings, given their uncoupled character and in general behave like the uncoupled modes of Figure 1c.

In Figure 1a the phonon branches are in general less dispersive than for $\kappa = 0$ in Figure 1c, especially for the coupled acoustic vibrations. This implies a reduction in the average group velocity and consequently in the phonon thermal conductivity, as pointed out in [12].

The r.h.s. of (14) as a function of $\cos(qd)$ could be plotted in the interval $[1, -1]$ –corresponding to the values of q in the interval $[0, \pi/d]$ –for a fixed value of κ . This kind of plot helps to obtain a quick view of the phonon modes for different values of κ as in Figure 1a.

The calculations of the present section with other 3D phenomenological discrete models [18] would imply a costly computation even compared with the diagonalization of the secular matrix our approach.

3.2 Strained Si/Ge superlattices

The purpose of this section is to study the phonon modes of short period strained Si/Ge SLs. The lattice constants and phonon frequencies of the strained bulk materials are employed as input parameters in the calculations (Tab. I of Ref. [10]). Matching to a $\text{Si}_{0.5}\text{Ge}_{0.5}$ substrate in the homogeneous strain configuration has been considered. For the Si acoustic modes we used the bulk sound velocities $v_L = 8.34 \times 10^5 \text{ cm s}^{-1}$ and $v_T = 5.90 \times 10^5 \text{ cm s}^{-1}$. For the Ge acoustic modes we fitted the bulk linear dispersion to a larger interval of the Brillouin zone in order to improve the results of the calculations, i.e. $v_L = 4.45 \times 10^5 \text{ cm s}^{-1}$ and $v_T = 2.50 \times 10^5 \text{ cm s}^{-1}$. In Figure 2 the dispersion relation in the directions [001] and [010] for a $(\text{Si})_8\text{-(Ge)}_8$ SL matched to a $\text{Si}_{0.5}\text{Ge}_{0.5}$ substrate is presented. With solid (dashed) lines we represent the modes that are pure L (T) in $\kappa = 0$. This structure could be compared with the strain-symmetrized SL intensively studied experimentally and theoretically with reliable first principle calculations in [15]. We find a good coincidence with our calculations. The phonons in the direction [001] was discussed in [10]. We limit our results in the $\Gamma\Delta$ direction to $1/4$ of the Brillouin zone ($1.14 \times 10^8 \text{ cm}^{-1}$) for the same reasons explained above. We did not find in the literature reports for other directions of the reciprocal space, although different 3D approaches have been set up, e.g. [18].

4 Conclusions

The phenomenological long-wavelength approach for atomic vibrations in nonpolar semiconductor heterostructures of reference [10] is studied both analytically and numerically for arbitrary directions of the reciprocal space without additional efforts respect to the high symmetry direction. The advantages compared with other theoretical models –given by the allowed analytical treatment and the facilities in the numerical computation– are shown. A simple expression for the dispersion relation in SL is found. It distinguishes between two different kinds of phonon modes related to the SL symmetry.

Numerical results for unstrained isotopic Ge SLs and QWs and strained Si/Ge SLs are presented. For isotopic SLs there is no other work to compare the phonon modes for the transverse wavevector $\kappa \neq 0$, but we obtain the expected results. We compare the results for a $(\text{Si})_8\text{-(Ge)}_8$ SL matched to a $\text{Si}_{0.5}\text{Ge}_{0.5}$ substrate with a sophisticated ab initio approach, and find a good agreement.

The wave nature of phonons was invoked in the past extrapolating, to the case of phonons, some mathematical developments for electrons [1]. The similarities between the dispersion relation for long wavelength phonons and

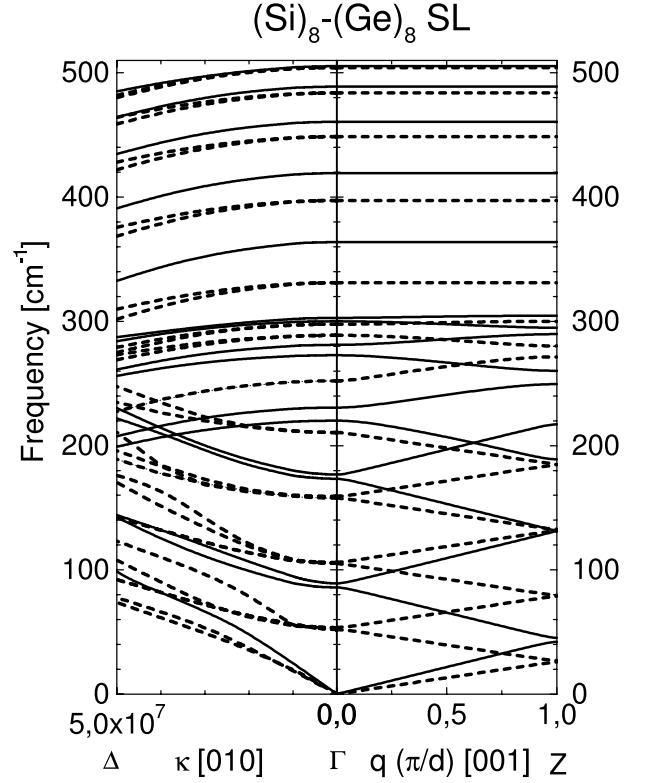


Fig. 2. Dispersion relation for the $(\text{Si})_8\text{-(Ge)}_8$ SL matched to a $\text{Si}_{0.5}\text{Ge}_{0.5}$ substrate in the direction [001]. The optical and acoustic L and T modes are plotted in the directions ΓZ and $\Gamma\Delta$. With solid (dashed) lines we represent the modes that are pure L (T) in $\kappa = 0$. See text for details.

the envelope functions for electrons was shown in reference [10]. The results obtained in this paper could be easily applicable in other problems where coupled wave solutions are found. Also generalization to include more coupled solutions could be possible.

We acknowledge F. Comas for clarifying discussions.

Appendix A: Elements of the secular matrix for the SL

The SL secular equation for the coupled modes can be written in the matrix form [10]:

$$\det \begin{pmatrix} A & B \\ C & D \end{pmatrix} = 0. \quad (25)$$

The order of the submatrices A , B , C and D is 4×4 . The diagonal submatrix A (D) contains only transverse (longitudinal) magnitude for $\kappa = 0$. On the other hand the non-diagonal submatrices C and B are responsible for the L-T mixing for $\kappa \neq 0$. The well (of width d_w) and barrier (of width d_b) materials are label as w and b respectively d

$$A = \begin{pmatrix} k_{Tw}S_{Tw} & -ik_{Tw}C_{Tw} & k_{Tb}S_{Tb} & ik_{Tb}C_{Tb} \\ \rho_w\beta_{Tw}^2r_wC_{Tw} & i\rho_w\beta_{Tw}^2r_wS_{Tw} & -\rho_b\beta_{Tb}^2r_bC_{Tb} & i\rho_b\beta_{Tb}^2r_bS_{Tb} \\ -e^{iqd}k_{Tw}S_{Tw} & -ie^{iqd}k_{Tw}C_{Tw} & -k_{Tb}S_{Tb} & ik_{Tb}C_{Tb} \\ e^{iqd}\rho_w\beta_{Tw}^2r_wC_{Tw} & -ie^{iqd}\rho_w\beta_{Tw}^2r_wS_{Tw} & -\rho_b\beta_{Tb}^2r_bC_{Tb} & -i\rho_b\beta_{Tb}^2r_bS_{Tb} \end{pmatrix}, \quad (21)$$

$$B = \begin{pmatrix} -S_{Lw} & iC_{Lw} & -S_{Lb} & -iC_{Lb} \\ -2b_{wT}k_{Lw}C_{Lw} & -2ib_{wT}k_{Lw}S_{Lw} & 2b_{bT}k_{Lb}C_{Lb} & -2ib_{bT}k_{Lb}S_{Lb} \\ e^{iqd}S_{Lw} & ie^{iqd}C_{Lw} & S_{Lb} & -iC_{Lb} \\ -2ie^{iqd}b_{wT}k_{Lw}C_{Lw} & 2ie^{iqd}b_{wT}k_{Lw}S_{Lw} & 2b_{bT}k_{Lb}C_{Lb} & 2ib_{bT}k_{Lb}S_{Lb} \end{pmatrix}, \quad (22)$$

$$C = \begin{pmatrix} iC_{Tw} & -S_{Tw} & -iC_{Tb} & -S_{Tb} \\ -2ib_{wT}k_{Tw}S_{Tw} & -2b_{wT}k_{Tw}C_{Tw} & -2ib_{bT}k_{Tb}S_{Tb} & 2b_{bT}k_{Tb}C_{Tb} \\ ie^{iqd}C_{Tw} & e^{iqd}S_{Tw} & -iC_{Tb} & S_{Tb} \\ 2ie^{iqd}b_{wT}k_{Tw}S_{Tw} & -2e^{iqd}b_{wT}k_{Tw}C_{Tw} & 2ib_{bT}k_{Tb}S_{Tb} & 2b_{bT}k_{Tb}C_{Tb} \end{pmatrix}, \quad (23)$$

$$D = \begin{pmatrix} ik_{Lw}C_{Lw} & -k_{Lw}S_{Lw} & -ik_{Lb}C_{Lb} & -k_{Lb}S_{Lb} \\ -i\rho_w t_w S_{Lw} & -\rho_w t_w C_{Lw} & -i\rho_b t_b S_{Lb} & \rho_b t_b C_{Lb} \\ ie^{iqd}k_{Lw}C_{Lw} & e^{iqd}k_{Lw}S_{Lw} & -ik_{Lb}C_{Lb} & k_{Lb}S_{Lb} \\ ie^{iqd}\rho_w t_w S_{Lw} & -e^{iqd}\rho_w t_w C_{Lw} & i\rho_b t_b S_{Lb} & \rho_b t_b C_{Lb} \end{pmatrix}, \quad (24)$$

and q are the superlattice period and wave vector respectively. The explicit expression for the submatrices are as follows

see equations (21–24) above,

where

$$S_{L_i(T_i)} = \sin\left(\frac{k_{L_i(T_i)}d_i}{2}\right), \quad C_{L_i(T_i)} = \cos\left(\frac{k_{L_i(T_i)}d_i}{2}\right), \quad (25)$$

$$r_i = (k_{T_i}^2 - \kappa^2), \quad b_{L_i(T_i)} = \rho_i \beta_{L_i(T_i)},$$

$$t_i = (\kappa^2 (\beta_{L_i}^2 - 2\beta_{T_i}^2) + \beta_{L_i}^2 k_{L_i}^2),$$

and $i = w, b$.

References

1. B. Jusserand, M. Cardona, *in Light Scattering in Solids V*, edited by M. Cardona, G. Güntherodt (Springer-Verlag, Heidelberg, 1989)
2. R. Tsu, S.S. Jha, *Appl. Phys. Lett.* **20**, 16 (1972); A.S. Barker, Jr. J.L. Merz, A.C. Gossard, *Phys. Rev. B* **17**, 3181 (1978)
3. For a recent review see S. Baroni, S. de Gironcoli, A. Dal Corso, P. Giannozzi, *Rev. Mod. Phys.* **73**, 515 (2001)
4. S.M. Rytov, *Akust. Zh.* **2**, 71 (1956) [*Sov. Phys. Acoust.* **2**, 68 (1956)]; C. Colvard, R. Merlin, M.V. Klein, A.C. Gossard, *Phys. Rev. Lett.* **43**, 298 (1980); B. Jusserand, F. Alexandre, J. Dubard, D. Paquet, *Phys. Rev. B* **33**, 2897 (1986); P. Santos, L. Ley, J. Mebert, O. Koblinger, *Phys. Rev. B* **36**, 4858 (1987)
5. S. Tamura, J.P. Wolfe, *Phys. Rev. B* **35**, 2528 (1987); S. Tamura, D.C. Hurley, J.P. Wolfe, *Phys. Rev. B* **38**, 1427 (1988); and references therein
6. S. Mizuno, S. Tamura, *Phys. Rev. B* **45**, 734 (1992); S. Mizuno, S. Tamura, *Jpn J. Appl. Phys.* **32**, 2206 (1993)
7. E.B. Christoffel, *Annu. Mater. Pura Appl.* **8**, 193 (1877); see also A.G. Every, *Phys. Rev. Lett.* **42**, 1065 (1979); A.G. Every, *Phys. Rev. B* **22**, 1746 (1980)
8. C. Trallero-Giner, F. García-Moliner, V.R. Velasco, M. Cardona, *Phys. Rev. B* **45**, 11944 (1992); for a more detailed presentation see C. Trallero-Giner, R. Pérez-Alvarez, F. García-Moliner, *Long wave polar modes in semiconductor heterostructures* (Pergamon/Elsevier Science, London, 1998)
9. F. Comas, R. Pérez-Alvarez, C. Trallero-Giner, M. Cardona, *Superlatt. Microstr.* **14**, 95 (1993); R. Pérez-Alvarez, V.R. Velasco, F. García-Moliner, *Physica Scripta* **51**, 526 (1995)
10. F. de León-Pérez, R. Pérez-Alvarez, *Phys. Rev. B* **61**, 4820 (2000)
11. F. de León Pérez, R. Pérez-Alvarez, *Phys. Rev. B* **62**, 9915 (2000)
12. F. de León-Pérez, R. Pérez-Alvarez, *Phys. Rev. B* **63**, 245304 (2001)
13. See F. García-Moliner, V.R. Velasco, *Theory of Single and Multiple Interfaces* (World Scientific, Singapore, 1992); V.R. Velasco, F. García-Moliner, *Surf. Sci. Rep.* **28**, 123 (1997) and references therein
14. J. Spitzer, T. Ruf, M. Cardona, W. Dondl, R. Schorer, G. Abstreiter, E.E. Haller, *Phys. Rev. Lett.* **72**, 1565 (1994); J. Spitzer, Ph.D. thesis, University of Stuttgart, 1994
15. S. de Gironcoli, E. Molinari, R. Shorer, G. Abstreiter, *Phys. Rev. B* **48**, 8959 (1993); R. Shorer, G. Abstreiter, S. de Gironcoli, E. Molinari, H. Kibbel, H. Presting, *Phys. Rev. B* **49**, 5406 (1994)
16. C. Trallero-Giner, F. Comas, *Philosophical Magazine B* **70**, 583 (1994)
17. R. Pérez-Alvarez, F. de León-Pérez, *Physica Scripta* **58**, 525 (1998)
18. R.A. Ghanbari, J.D. White, G. Fasol, C.J. Gibbings, C.G. Tupper, *Phys. Rev. B* **42**, 7033 (1990); M.I. Alonso, M. Cardona, G. Kanellis, *Solid State Commun.* **69**, 479 (1989)